TELKOMNIKA, Vol. 11, No. 5, May 2013, pp. 2442 ~ 2447
ISSN: 2302-4046

Raman Slow Light in Distributed Raman Fiber Sensors

Dapeng Wang*, Ning Li, Aimei Yan, Yingxin Xie, Fengyu Wang
Beijing Guodiantong Network Technology Co., LTD., Nari Group Corporation, Beijing 100120, China.
Corresponding author, e-mail: bupt_wae@sina.com, li-ning@ sgepri.sgcc.com.cn, yanaimei@sgepri.sgcc.com.cn, xieyingxin@sgepri.sgcc.com.cn, wangfengyu@sgepri.sgcc.com.cn

Abstract

Distributed Raman sensor offers a number of advantages to the implementation of smart grid, which is aimed to improve reliability and energy efficiency as compared with traditional power grid. However, the fantastic properties of slow light are rarely considered in the former studies on the Raman sensor systems. In this paper, the effects of Raman slow-light on room-temperature single-mode optical fiber sensors are examined by extracting the Raman pulse-delay terms from extended nonlinear Schrodinger equation (NLSE). Numerical study shows that pulse parameters such as pulse position, frequency chirp, and envelope distortion may be greatly affected by slow light. Two important points of pump power are show clearly keeping the Raman pulse zero walk-off or chirp free, respectively. We demonstrate a method based on pump power adjustment for compensating the slow light induced impairment.

Keywords*: fiber sensor, slow light, stimulated Raman scattering, chirp, smart grid*

1. Introduction

Distributed fiber sensor is of critical importance in many applications measuring strain, temperature, pressure and other quantities [1-5]. Smart grid, which is aimed to improve reliability and energy efficiency as compared with traditional power grid, employs fiber sensors as the information interface. In the past years, distributed Raman sensors have been widely researched and various schemes have been proposed for high-accuracy, high-spatial-resolution measurements to meet the requirements of smart grid.

Recently, the groundbreaking of achieving slow and superluminal light propagation velocity have caused keen interest of slow and fast light [6-12]. In fiber sensors, both stimulated Raman scattering (SRS) and stimulated Brillouin scattering (SBS) can introduce strong group velocity dispersions [4-6] to slow down the light speed at room temperature. The slow light based on SBS has a restricted bandwidth about GHz and SRS allows data rates up to nearly terabits per second due to the Raman resonance width [6], [8]. It is quite important to survey the effects of Raman slow light on sensors for the future applications.

In this paper, we demonstrate theoretically that slow light affects pulse parameters such as pulse position, frequency chirp, and envelope distortion. All the effects are derived from Raman resonance of the fiber. The walk-off enlarged by slow light expedites the gain saturation. When the pump pulse attenuated enough the group delay will also be dulled. These studies are mainly towards to the detailed character of high resolution distributed Raman fiber sensors for the potential applications in smart grid.

2. Research Method

Raman scattering is the process by which energy transferred from high frequency components of optical field to the lower frequency components in the dielectric media. This amplification of lower frequency components is associated with the dressing of medium refractive index under the constraint of causality. The character of Raman scattering is decided by the Raman susceptibility. Raman susceptibility χ_R is a complex function of frequency which has been well studied in SiO_2 glasses. The imaginary components χ'' of χ_R related to the Raman gain profile can be measured by the experiments, and then the real components

Received January 15, 2013; Revised March 9, 2013; Accepted March 18, 2013

χ' related to the effective refractive index $n(\omega)$ near Raman resonance can be obtained from χ'' lying in the requirement of the so-called Kramers–Kronig relation. A commonly used assumption is that the frequency dependence of the Raman susceptibility is linear. One can calculate the Raman scattering-induced time delay as [6]

$$\Delta t = L(\frac{1}{v_g} - \frac{1}{v_{fg}}) = \frac{gIL}{\Delta\omega_R} \quad (1)$$

where g is the steady-state Raman gain, L is the length of medium, I is the pump intensity, v_g is the group speed of stokes wave, v_{fg} is the background group speed and $\Delta\omega_R$ is the gain linewidth. Thus the group velocity of the pulse with pump is

$$v_g = (\frac{gI}{\Delta\omega_R} + \frac{1}{v_{fg}})^{-1} \quad (2)$$

To reveal the origin of time delay in theoretically, we assume that the pump experiences a negligible depletion, thus the differential equation of Raman response is

$$\frac{\partial A_s}{\partial z} = i\gamma_s f_R A_p \int_{-\infty}^{\infty} R(t-t')A_s(t')A_p^*(t')\exp(i\omega_R(t-t'))dt' \quad (3)$$

where A_p and A_s are the pump and stokes field respectively. Considering the interaction of a cw pump wave with a pulsed signal, for the following theory, we assume that the pump experiences a negligible depletion as a result of the interaction with the pulse signal. The well-known relation for the amplitudes and phases in the Raman interaction reads as

$$\frac{\partial A_s}{\partial z} = i\gamma_s f_R I_p \int_{-\infty}^{\infty} R(t-t')A_s(t')\exp(i\omega_R(t-t'))dt' \quad (4)$$

where $I_P = |A_p|^2$ is the pump intensity.

In frequency domain, the stokes field can be expressed as

$$A_s(\omega, L) = |H(\omega)|\exp(i\Phi(\omega))A_s(\omega, 0) \quad (5)$$

where $|H(\omega)| = \exp(z\gamma_s f_R I_P \chi''(\omega-\omega_R))$, and $\Phi(\omega) = z\gamma_s f_R I_P \chi'(\omega-\omega_R)$ is the amplitude and phase transfer function, respectively. The group delay is then calculated by

$$\tau = -\frac{\partial\Phi(\omega)}{\partial\omega} = -z\gamma_s f_R I_P \frac{\partial\chi'(\omega-\omega_R)}{\partial\omega} \quad (6)$$

We quote the definition the gain coefficient $g_s = 2\gamma_s f_R f_0$ and the inverse of group velocity $v_{gR}^{-1} = -\gamma_s f_R I_p f_1$, f_n are the n-th Taylor series coefficients of Raman susceptibility. The signal is finally described as

$$\frac{\partial A_s}{\partial z} + (v_{fg}^{-1} + v_{gR}^{-1})\frac{\partial A_s}{\partial t} + \frac{i\beta_{2s}}{2}\frac{\partial^2 A_s}{\partial t^2} = \frac{g_s}{2}|A_p|^2 A_s + i\gamma_s(|A_s|^2 + (1-f_R)|A_p|^2)A_s \quad (7)$$

where β_{2s} is the group velocity dispersion (GVD) coefficient of signal pulse. The high order coefficients ($n \geq 3$) are omitted.

Eq. 7 provides the approximate relationship between the imaginary (gain) and the real (phase) part of Raman susceptibility. Raman pulse group speed change is decided by the gain change according to this relationship.

We adopt the coupled NLSE to study the characters of pulse walk-off. The group delay of Raman pulse relates to the pump power I besides the fiber parameters such as g, L, which means the depletion of pump pulse will deduce the delay time impairment.

3. Results and Analysis

To illustrate the dynamic properties of light slow down, we deliberately choose the optical fiber parameters in a highly nonlinear hollow-core photonic crystal fiber filled with carbon disulfide [12] to fulfill the magnitude of walk-off compensation required. The parameters are pulse width $T_0 = 5ps$, nonlinear coefficient $\gamma = 0.01m^{-1}W^{-1}$, walk-off length $L_w = 20m$, fiber length $L = 2km$, Raman frequency detuning $\Omega / 2\pi = 7.5THz$, effective core area $A_{eff} = 20\mu m^2$, GVD coefficient $\beta_2 = 20\,ps^2 / km$, Raman gain $g = 10^{-13} m / W$. The effects of slow light on the pulse walk-off and chirp are then studied numerically and compared with the condition without slow light.

3.1. Slow Light Effects on Walk-Off and Frequency Chirp

Figure 1. shows how walk-off decreases with the pump power increase by the slow light effect, though it is usually considered as a constant depicted by the blue curve. In the small signal condition, the pump power is much stronger than the signal, thus the depletion of the pump is negligible. The pulse walk-off decreases directly with the pump power increase as is described by the red curve. This relation is simple but should be revised when the pump power is strong enough because of the slow light effect. It's interesting that the numerical results show a turning point at the pump power about 1.55W as is depicted by the black curve, deviating from the analytical prediction. We define this point as the minimum walk-off initial power. Pulse walk-off can be abated completly in the well chosen fiber system.

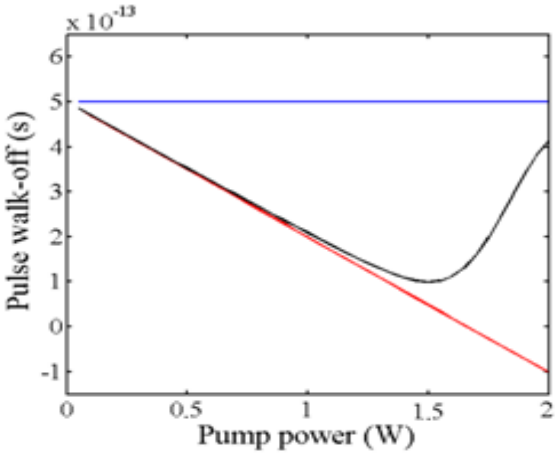

Figure 1. Pulse walk-off as a function of the pump power. Blue curve, without slow light. Red curve, analytical results in the undepleted condition. Black curve, numerical results.

As is researched, the total frequency chirp across the signal pulse can be full controlled by tuning the pump power for its dependence on slow light. The chirp decreases when the pump power increase without the effect of slow light, as the blue curve in Figure 2 shows. The

red curve describes that the pulse chirp increases rapidly when the pump power grows stronger, as the analytical results of small signal condition predicted. We provide more details of chirp at the pump exhaustion region. When the energy of pump pulse is transfered to the signal enough the chirp also has a turning point as is shown by the black curve. It is clearly that the frequency chirp with or without slow light have opposite sign at most time, and Raman pulse is nearly chirp free at low pump power region compared to the non-slow-light condition. The chirp has a positive maximum value, which intimates another chirp free point. And the Raman gain is finally saturated in the high pump area, which is reasonable considering the slow light effect on the frequency chirp.

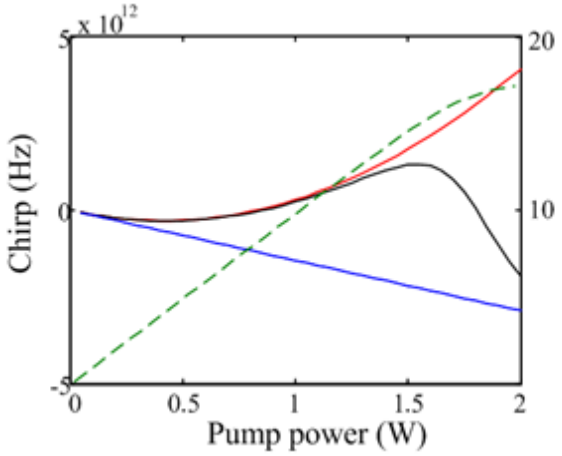

Figure 2. Pulse frequency chirp as a function of the pump power. Blue curve, without slow light. Red curve, analytical results in the undepleted condition. Black curve, numerical results. Green curve, numerical results of final Raman gain.

3.2. Optical Fields Propagation in Fiber with/without Slow Light

Numerical simulation results based on coupled wave equation is shown in Figure 3. This figure shows both the intensity and frequency distribution without considering the slow light effect. The sign of the group velocity dispersion also affects the field distribution, and we discuss normal dispersion in this paper only.

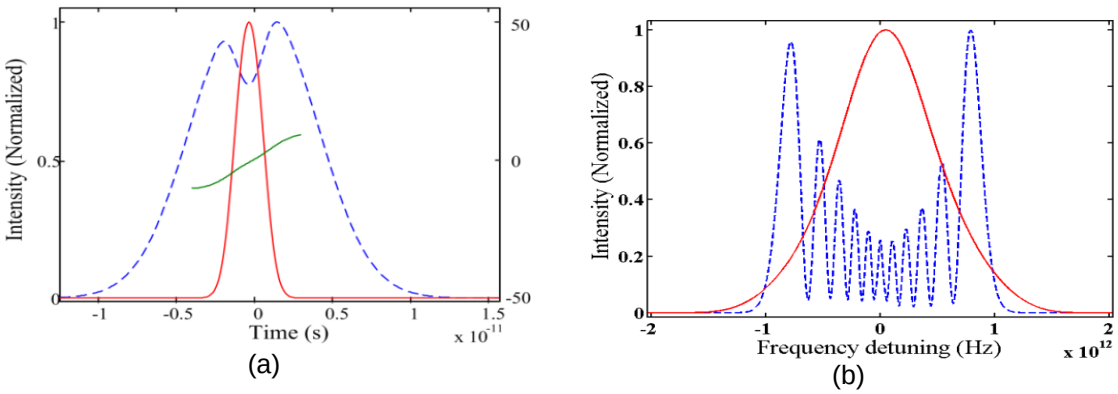

Figure 3. Pump (blue, dashed) and signal (red, solid) without slow light after propagation. (a) Profiles in time domain. (b) Frequency spectrum.

Raman pulse moves to the leading edge of the pump pulse in the normal dispersion region. The walk-off between the pump and the signal is fixed without slow light, thus the energy

is transferred mainly from the low frequency components of the pump pulse as is shown in Figure 3(a). The pump spectrum becomes asymmetrical as the pump attenuated in the leading side, as is shown in Figure 3(b). It could be futher found that the signal pulse is low distorted compared with the pump. The green curve is the Raman pulse chirp (THz).The zero frequency chirp point arises at Raman pulse trailing edge rather than the peak.

Assuming pump power equals about 1.7W, the group velocity mismatch induced walk-off can be canceled by the slow light effect as is shown in Figure 4. Group-velocity matching between the two pulses makes slow light exactly compensating the group-velocity dispersion. Raman pulse is exactly synchronous with the pump pulse, connoting a low distortion. In this condition the pulse shapes both in time and frequency domain are all well shaped, as Figure 4(a) and Figure 4(b) show respectively.

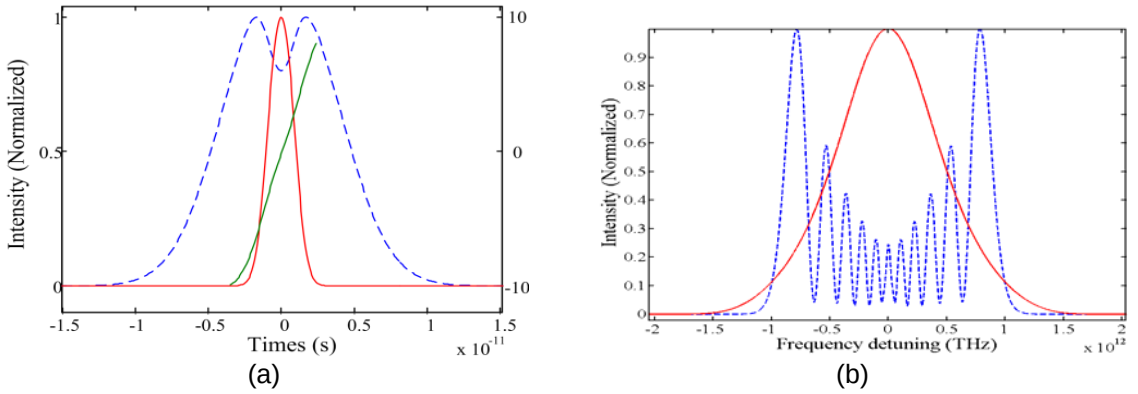

(a) (b)

Figure 4. Pump (blue, dashed) and signal (red, solid) with slow light after propagation at zero walk-off power. (a) Profiles in time domain. (b) Frequency spectrum.

The green curve in Figure 4(a) shows that the zero frequency chirp point moves to the leading edge of Raman pulse, which means the pulse chirp is not equal to zero nearly in the most time. This deviation from the pulse peak could be interpreted as the influence of the cross phase modulation.

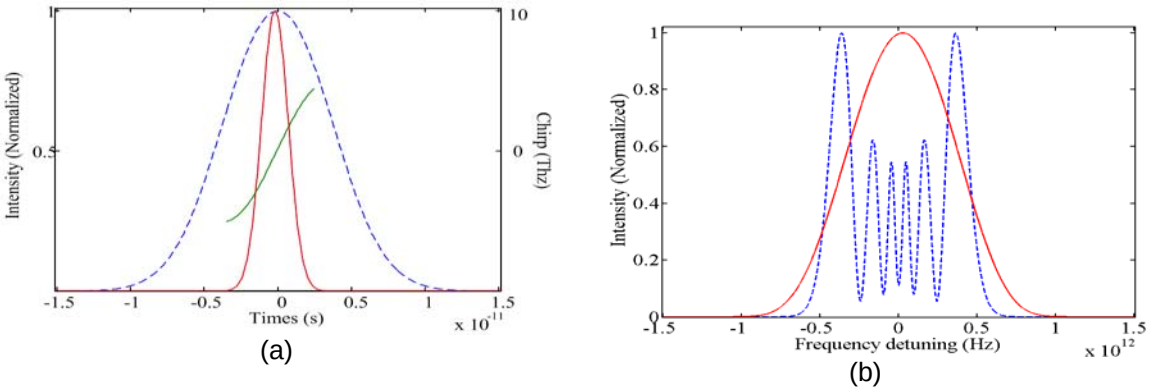

(a) (b)

Figure 5. Pump (blue, dashed) and signal (red, solid) with slow light after propagation at zero chirp power. (a) Profiles in time domain. (b) Frequency spectrum.

Adjusting the pump power to 0.85W can synchronize the effects related and change the zero frequency chirp point as is shown in Figure 5(a). The distortion of pump and signal frequency spectra are also described by Figure 5(b). Raman pulse walks back to the leading edge of the pump when the group velocity mismatch emerges again. Fortunately, the change of

envelope is slightly compared with the zero walk-off condition. The pulse peak centered absence of chirp can be interpreted as the group and phase velocity nearly having the same variation tendency. Except the condition mentioned above, frequency shift always exists across the whole Raman pulse. And the independence between the propagates speed of signal phase and signal envelope resulting the chirp leading or lagging the pulse position which is modified by the tuning of walk-off. The group and phase velocity nearly have the same variation tendency, thus the pulse peak is chirp free.

The effect of the pulse walk-off gives rise to the pulse delay or advancement in cw pump sensor. It should be noticed that the pulse chirp ultimately affect on the optical field intensity. Slow light primarily influences the signal pulse position in the small signal and cw pump condition. The delay of signal pulse enhances the energy amplification and shortens the fiber effective length when the pump depletion is not negligible. As to the pulsed pump, the depletion is related to the walk off. Gain saturation degrades the performance of the sensor when the pump power is strong enough.

4. Conclusion

In conclusion, we have demonstrated the effects of Raman slow-light on room-temperature single-mode optical fiber sensors by extracting the Raman pulse-delay terms from extended nonlinear Schrodinger equation. The gain saturation cuts down the flexibility of the sensor. The compensation can be achieved in a well chosen system by adjusting the pump power.

References

[1] Ukil A, Braendle H, Krippner P. Distributed Temperature Sensing: Review of Technology and Applications, *Sensors Journal, IEEE*. 2012; 12: 885.
[2] Jonghan Park Bolognini G, Duckey Lee, Pilhan Kim , Pilki Cho, Di Pasquale F, Namkyoo Park. Raman-based distributed temperature sensor with simplex coding and link optimization. *Photonics Technology Letters, IEEE*. 2006; 18: 1879.
[3] De Leonardis, F Passaro, VMN. Modeling and Performance of a Guided-Wave Optical Angular-Velocity Sensor Based on Raman Effect in SOI. *Journal of Lightwave Technology*. 2007; 25: 2352.
[4] Luc Thevenaz and Kwang Yong Song. Time biasing due to the slow-light effect in distributed fiber-optic Brillouin sensors. *Opt. Lett*. 2006; 31: 715.
[5] Lufan Zou, Xiaoyi Bao, Shiquan Yang, Liang Chen, and Fabien Ravet. Effect of Brillouin slow light on distributed Brillouin fiber sensors. *Opt. Lett*. 2006; 31: 2698.
[6] Gil Fanjoux and Thibaut Sylvestre. All-optical tunable pulse frequency chirp via slow light. *Opt. Lett*. 2009; 34: 3824.
[7] K Lee and NM Lawandy. Optically induced pulse delay in a solid-state Raman amplifier. Appl. *Phys. Lett.* 2001; 78: 703.
[8] JE Sharping, Y Okawachi, and AL Gaeta. Wide bandwidth slow light using a Raman fiber amplifier. *Opt. Express*. 2005; 13: 6092.
[9] D Dahan, A Bilenca, and G Eisenstein. Noise-reduction capabilities of a Raman-mediated wavelength converter. *Opt. Lett.* 2003; 28: 34.
[10] G Fanjoux and T Sylvestre. Cancellation of Raman pulse walk-off by slow light. *Opt. Lett.* 2008; 33: 2506.
[11] G Fanjoux, J Michaud, H Maillotte, and T Sylvestre. Slow-Light Spatial Solitons. *Phys. Rev. Lett.* 2008; 100: 013908.
[12] S Lebrun, P Delaye, R Frey, and G Roosen. High-efficiency single-mode Raman generation in a liquid-filled photonic bandgap fiber. *Opt. Lett*. 2003; 32: 337.